Biosensors and Bioelectronics 188 (2021) 113338

Contents lists available at ScienceDirect

Biosensors and Bioelectronics

journal homepage: www.elsevier.com/locate/bios

Development of an advanced DNA biosensor for pathogenic *Vibrio cholerae* detection in real sample

M.R. Ali [a,b], M.S. Bacchu [a,b], M.A.A. Setu [c], S. Akter [c], M.N. Hasan [a,b], F.T. Chowdhury [d], M. M. Rahman [e], M.S. Ahommed [f], M.Z.H. Khan [a,b,*]

[a] Dept. of Chemical Engineering, Jashore University of Science and Technology, Jashore, 7408, Bangladesh
[b] Laboratory of Nano-bio and Advanced Materials Engineering (NAME), Jashore University of Science and Technology, Jashore, 7408, Bangladesh
[c] Dept. of Microbiology, Jashore University of Science and Technology, Jashore, 7408, Bangladesh
[d] Dept. of Chemistry, University of Rajshahi, Rajshahi, 7205, Bangladesh
[e] Dept. of General Educational Development (GED), Daffodil International University, Mirpur Road, Dhanmondi, Dhaka, 1207, Bangladesh
[f] Dept. of Chemistry, Graduate School of Science, Tohoku University, Aoba-ku, Sendai, 980-8578, Japan

ARTICLE INFO

Keywords:
DNA biosensor
Vibrio cholerae
Electrochemical detection
APTES/NHS matrix
Poultry feces

ABSTRACT

Due to the epidemics of emerging microbial diseases worldwide, the accurate and rapid quantification of pathogenic bacteria is extremely critical. In this work, a highly sensitive DNA-based electrochemical biosensor has been developed to detect *Vibrio cholerae* using gold nanocube and 3-aminopropyltriethoxysilane (APTES) modified glassy carbon electrode (GCE) with DNA carrier matrix. Electrochemical impedance spectroscopy (EIS), cyclic voltammetry (CV), Fourier transform infrared spectroscopy (FTIR), scanning electron microscope (SEM) experiments were performed to interrogate the proposed sensor at each stage of preparation. The biosensor has demonstrated high sensitivity with a wide linear response range to target DNA from 10^{-8} to 10^{-14} ($R^2 = 0.992$) and 10^{-14} to 10^{-27} molL^{-1} ($R^2 = 0.993$) with a limit of detection (LOD) value of 7.41×10^{-30} molL^{-1} ($S/N = 5$). The biosensor also exhibits a selective detection behavior in bacterial cultures that belong to the same and distant genera. Moreover, the proposed sensor can be used for six consecutive DNA assays with a repeatability relative standard deviations (RSD) value of 5% ($n = 5$). Besides, the DNA biosensor shows excellent recovery for detecting *V. cholerae* in poultry feces, indicating that the designed biosensor could become a powerful tool for pathogenic microorganisms screening in clinical diagnostics, food safety, and environmental monitoring.

1. Introduction

Cholera is a virulent diarrheal disease that became an international priority and intimidating concern for public health. This enteric concern poses a substantial threat to humanity due to having emerging mortality scenarios worldwide (Hall-Stoodley et al., 2004). Cholera is a well-known epidemic disease caused by the infection of gram-negative bacterium called Vibrio Cholerae (Faruque et al., 1998). Based on the O-antigen classification, more than 200 serogroups were identified for this anaerobic bacterium. Still, only O1 and O139 were the most effective pathogenic strains responsible for the infection in the human body around various regions (Chowdhury et al., 2016; Shin et al., 2011). These toxigenic strains exist in aquatic ecosystems as natural inhabitants and form biofilm on abiotic surfaces (Teschler et al., 2015). Though infections begin with edible food or water contaminated with the specified bacterium, *V. cholerae* has easy access to direct transmission between humans. The countries with the most natural disasters and low-middle-income countries are the primary sufferers due to unsafe water and poor sanitation. The most frightening part is that this disease is often associated with mild symptoms like vomiting and dehydration but can be severe afterward (Andrews and Basu, 2011; Weil et al., 2009). From 2008 through 2012, researchers estimated about 1.3–4.0 million new cases and 21,000 to 143,000 deaths per year as a result of that life-threatening illness in 51 countries, and the number of cases-deaths ratios increased by near about 50% (Ali et al., 2015; Harris et al., 2012). World Health Organization (WHO) notified 923,037 new cases and 1911 deaths from 31 countries in 2019. Therefore, reliable rapid diagnostics tool has always been an imperative need for controlling and preventing the consequences of the outbreak by early and accurate detection (Ross et al., 2015).

* Corresponding author. Dept. of Chemical Engineering, Jashore University of Science and technology, Jashore, 7408, Bangladesh.
E-mail address: zaved.khan@just.edu.bd (M.Z.H. Khan).

https://doi.org/10.1016/j.bios.2021.113338
Received 21 April 2021; Received in revised form 10 May 2021; Accepted 11 May 2021
Available online 15 May 2021

The most common traditional approach was the culture method following biochemical test identifications, which is still considered the gold standard of cholerae diagnostics. It worked by isolating the target bacteria from stool samples on suitable selective mediums following serological marker with particular antibodies (Alam et al., 2010). Other traditional methods include gel electrophoresis (Cooper et al., 2006), lateral flow (Yu et al., 2011), enzyme-linked immunosorbent assay (ELISA) (Ramamurthy et al., 1992), and quartz crystal microbalance (QCM) (Carter et al., 1995) are reported so far. Although these were timely solutions and proven to be efficient methods, these techniques are time-consuming, labor-intensive, and difficult to prepare linked materials. Later, several molecular-based detection methods were developed, including polymerase chain reaction (PCR) (Goel et al., 2007), latex agglutination assays (Yamazaki et al., 2008), loop-mediated isothermal amplification (LAMP) (Okada et al., 2010), molecular rapid diagnostic tests (mRDTs) (Huq et al., 2012), immunofluorescence (Aulet et al., 2007), and DNA microarray (Liu et al., 2006). However, these techniques have long served but have limited use in real-time mobile monitoring due to sophisticated instrumentations, high experimental cost, long detection time, and mainly require highly skilled personnel.

Over the past few years, electrochemical DNA biosensors grabbed substantial attention in the research community as an ideal alternative technique for pathogens detections. It has inherent advances like simple instrumentation, low cost, high sensitivity, signal stability, miniaturization, compatibility with micro-fabrication processes, and real sample detection. In a typical biosensor, a transducer converts the biological reaction between the bioreceptor and a specific target as a readable electrical signal proportional to the particular target concentration (Kumar et al., 2018). DNA biosensors are generally composed of single-strand DNA (ssDNA) known as a probe. The hybridization with analyte molecules following assigned transducer, e.g., pencil graphite electrodes (PGE), screen printed electrodes (SPE), gold electrodes (GE), GCE electrodes (Ulianas et al., 2014; Xu et al., 2017).

Yu et al. developed a *V. cholerae* enzymatic electrochemical biosensor using the thiolated anti-fluorescein-conjugated alkaline phosphatase (anti-FCAP)-labeled DNA probe immobilized on the gold SPE (Yu et al., 2015). The enzyme-catalyzed its α-naphthyl phosphate into electroactive-naphthalene to acquire DNA hybridization. However, this DNA hybridization is time-consuming, and the amperometric measurement can be performed only after labeling DNA hybrids with α-naphthyl phosphate. Previously, Patel et al. also reported an electrochemical DNA biosensor to detect *V. cholerae*, where methylene blue (MB) was used as the electroactive indicator to amplify the reaction signal (Patel et al., 2010). However, applications of the sensor in medical samples are usually limited by its weak response to low concentrations.

Various nanomaterials were reported to use for bio-receptors immobilization on electrode surface to upgrade the electroanalytical performance of sequence-specific detection of biorecognition elements (ssDNA) (Rashid and Yusof, 2017). In particular, gold nanoparticles (AuNPs) are often applied in biosensing applications to improve sensitivities, excellent signal response speed, adsorption ability of lower-concentration biological active molecules on the modified electrode (Khan et al., 2020; Zheng et al., 2019). Earlier, Liew et al. and Rahman et al. employed AuNPs in hybridization assay as the immobilization substrate to detect *V. cholerae*. Nonetheless, these techniques are bounded to PCR products, and LOD are limited to femto and zepto molar level, respectively (Liew et al., 2015; Rahman et al., 2017). Due to some attractive properties like monodisperse size, long shelf lives, and high surface reactivity, cubic-shaped gold nanoparticles (AuNC) can be highly conjugate with bioreceptor by functionalizing and stabilizing the immobilization surface (Ringe et al., 2010). A linker molecule can play a controlling part in anchoring the probe DNA for the hybridization process (Kurinomaru et al., 2019). For instance, APTES is frequently used in DNA biosensor for surface functionalization because of its active end group and stability in harsh conditions, increasing the efficiency and accuracy of hybridization (probe DNA-target sequence) concerning signals to noise ratio and reproducibility (Li et al., 2001).

In this work, we are reporting a sensitive electrochemical DNA biosensor for *V. cholerae* detection using a gold nanocube modified glassy carbon electrode as the DNA probe immobilization platform. 3-aminopropyltriethoxysilane/N-hydroxysuccinimide (APTES/NHS) chemistry was used as a coupling reagent for improving the immobilization efficiency. A particular immobilized DNA probe recognizes the nucleotide sequences (5′ to 3′) by the hybridization reaction followed by a signal/reporter probe of the most prevalent bacterium causing cholera infection. The detection event was monitored using a well-known labeling chemical anthraquinone-2-sulfonic acid monohydrate sodium salt (AQMS). The use of gold nanocube-modified glassy carbon electrodes treated by APTES/NHS coupling reagents improved the DNA binding capacity of the surface and sensitivity of the proposed biosensor. The sensor demonstrated exceptional performance in terms of sensitivity and detection limit compared to the other reported methods. We believe our study will bring new insight towards laboratory-based biosensor development and miniaturized-portable applications.

2. Materials and methods

2.1. Instruments

An electrochemical workstation of Corrtest CS300 was used to conduct all voltammetric measurements. Electrochemical impedance spectroscopy measurement was performed by using Metrohm DropSens μStat-i 400s. A conventional three-electrode system containing different modified glassy carbon electrodes as a working electrode, silver/silver chloride (Ag/AgCl) electrode as a reference electrode, and platinum wire as a counter electrode were employed during the electrochemical measurement. The surface topographical analyses were conducted by using ZEISS Gemini SEM 500 and NICOLET iS20 attenuated total reflection Fourier transform infrared (ATR-FTIR) spectroscopy.

2.2. Reagents

Chloroauric acid ($HAuCl_4$), ascorbic acid (AA), silver nitrate ($AgNO_3$), N-Hydroxysuccinimide, anthraquinone-2-sulfonic acid monohydrate sodium salt, 3-aminopropyltriethoxysilane, and polyvinyl pyrrolidone (PVP) were purchased from Sigma Aldrich (China). Potassium chloride (KCl), potassium ferrocyanide ($K_4[Fe(CN)_6]$), potassium ferricyanide ($K_3[Fe(CN)_6]$), and other reagents were brought from Merck (India). Ultrapure water (Type I) obtained from Evoqua was used to prepare all solutions. A phosphate buffer saline of 0.01 $molL^{-1}$ of pH 7.4 supplied by Aladdin reagents (Shanghai, China) was used as supporting electrolytic solution and washing solution. The strands of capture probe (VCvrra-CP), linear target (VCvrra-LT), reporter probe (VCvrra-RP), bases mismatch, and non-complementary linear target (NCLT) were purchased from Sangon Biotech (Shanghai, China). The nucleotide sequences (5′ to 3′) are listed below-

VCvrra-CP – GAACCAAATTTGACGGCCAG.

VCvrra-LT

- TGGCCGTCAAATTTGGTTCACTTGTGTACGCCCAAAGCC.

VCvrra-RP - GGCTTTGGGCGTACACAAGT.

One base mismatched

-TGGCCGTCAAATTTGCCACACTTGTGTACGCCCAAAGCC.

Two base mismatched

- TGGCCGTCAAATTTGCCAAGTTTGTGTACGCCCAAAGCC.

NCLT- GCCCAAACATCCATAGTACTGACATTTCGTCGACCGGACG.

2.3. Preparation of AuNC

In this study, a simple one-pot method was followed to synthesis uniformly cube-like AuNC. Firstly, PVP of 24 mg was dissolved in 12 ml water and stirred in the solution for 3 min. After that, 15 μl of 3 $molL^{-1}$

$HAuCl_4$ was added to 6 ml of 0.5 molL^{-1} $AgNO_3$ solution with continuously stirring. Later, an aqueous solution of 0.2 molL^{-1} AA was added and further stirred at 92.4 °C for 1hr. After completing the reaction, the solution was cooled, and the unreacted substance was separated by centrifuging with ultrapure water and ethanol several times.

2.4. Fabrication of GCE/AuNC/APTES

The GCE electrodes were mirror polished with 1, 0.3, and 0.05 μm of alumina slurry on microporous cloth. Later, the electrodes were rinsed off with ultrapure water and ultrasonically cleaned with ethanol for 3 min. Subsequently, pretreated the GCE surface with 1 molL^{-1} sulfuric acid (H_2SO_4) by cyclic voltammetry (CV) from −1.0 V to 1.0 V for 23 cycles with an optimum scan rate (0.1 V^{-1}) and rinsed again with ultrapure water. Before modification, treated GCE was dried well by nitrogen gas. GCE/AuNC has fabricated via drop-casting an aliquot (5 μl) of previously prepared AuNC suspension onto the surface of GCE and drying at room temperature under N_2 atmosphere. Furthermore, we followed the modification of APTES on the surface of GCE/AuNC as previously reported work (Khan et al., 2018).

2.5. Fabrication of DNA biosensor

Firstly, GCE/AuNC/APTES was immersed in 5 × 10^{-3} molL^{-1} NHS solution for stabilizing amine-reactive ester for binding amine group of the LT on the surface of GCE/AuNC/APTES and rinsed with ultrapure water to remove excess NHS. A passive adsorption method was applied for the immobilization of capture probe, complementary target, and reporter probes on GCE/AuNC/APTES/NHS surface by following the previously reported method (Rahman et al., 2017). In this process, the modified electrode was dipped into 5 × 10^{-6} molL^{-1} capture probe solution in 0.01 molL^{-1} PBS at 4 °C. After nightlong immobilization, rinsed the electrode with 0.01 molL^{-1} PBS and immersed into different concentration of LT in 0.01 molL^{-1} PBS containing 5 × 10^{-3} molL^{-1} AQMS solution to hybridize LT with CP. After completing 1 h hybridization, the GCE/AuNC/APTES/NHS/CP/LT was washed with 0.01 molL^{-1} PBS and dipped into 5 × 10^{-3} molL^{-1} solution of AQMS containing 1 × 10^{-6} molL^{-1} RP to fulfill the DNA hybridization. Finally, the electrode was washed with 0.01 M PBS for removing non-immobilize RP and ready for electrochemical measurements.

2.6. Electrochemical measurement

2.6.1. Electrochemical characterization

The CV characterization of different modified electrodes was done in 5 × 10^{-3} molL^{-1} $[Fe(CN)_6]^{3-/4-}$ containing 0.1 M KCl at a potential range of −0.2 V–0.6 V with a scanning rate of 50 mV/s. EIS studies were performed in the same solution at a frequency range of 100 kHz to 0.1 Hz with an applied voltage of 0.25 V. Specificity experiment of the biosensor was performed using one base mismatch, two base mismatch, and NCLT as control oligonucleotide sequences.

2.6.2. Voltammetric detection of Vibrio cholerae (VC)

DPV analyses were performed in the presence of 5 × 10^{-3} molL^{-1} AQMS as a redox indicator in 0.01 molL^{-1} PBS to detect VC. The condition of DPV measurements was initial potential −1 V, end potential 0 V, pulse width 50 ms, modulation 50 mV, and pulse period 0.1 s.

2.7. Preparation of real sample

We used bacterial isolates belong to *Vibrio cholerae* and Vibrio *mimicus* from the bacterial culture collection of the Department of Microbiology, Jashore University of Science and Technology as positive controls. Those strains were isolated from local barramundi fish (*Lates calcarifer*) collected from the estuary at the Sundarban area. Skin swab, portion of gill and intestinal contents of freshly caught fish were poured into Alkaline peptone water (Oxoid, UK) to enrich vibrios and transported to the laboratory within 6 h. One loopful of the both were streaked on thiosulphate-citrate-bile salts-sucrose (TCBS) media and incubated for 18 h at 37 °C (Baron et al., 2007). We screened the isolates by the colony morphology (yellow colony for *Vibrio cholerae* and green for Vibrio *mimicus*) and identified by API 20E biochemical profiling (Biomerieux, USA). However, these two species are closely related biochemically. We confirmed the identification by a multiplex polymerase chain reaction of sodB gene *and* sequencing of target genes using primers reported earlier (Tarr et al., 2007). We used reference bacterial strains, *Salmonella enterica* serovar Typhimurium (American type culture collection, ATCC, 19585) and Enterobacter aerogenes (ATCC 49469), as negative controls for analysis of selectivity of DNA biosensor. We extracted DNA using an extraction kit (QuickExtract™ DNA Extraction Solution, Lucigen, USA) following the manufacturer's instructions. In short, one loop-full of a pure overnight culture of the bacteria on Muller Hinton agar (OXOID, UK) is suspended in 500 μl of deionized (DNase/RNAse free) water and vortexed vigorously. The suspension was centrifuged, resuspended the pellet in 100 μl of extraction buffer (deionized water and DNA extraction buffer in 1:1 solution), and mixed well. Incubation of the suspension was carried out at 65 °C for 15 min and stored for further work at −20 °C. We measured the dsDNA concentration using a Nanodrop spectrophotometer and adjust the concentration at 5 ng/ml. The diluted dsDNA solution was heated at 100 °C for 10 min and instantly cooled on ice to prepare the ssDNA target. We allowed the bacterial ssDNA to hybridize the probe on the electrode surface at 53 °C (hybridization temperature calculated based on melting temperature of the DNA probe used on electrode) with the presence of AQMS.

Besides taking pure bacterial culture as the source of DNA, we also evaluated the recovery of bacterial DNA spiked in poultry feces. We took 100 mg untreated poultry feces in 1 ml deionized water and mixed it homogenously. 180 μl of the resulting suspension was spiked with 20 μl aliquots of the known bacterial suspension. Extraction of dsDNA and preparation of ssDNA followed the methods described previously.

3. Results and discussions

3.1. Surface topographical analysis of GCE/AuNC/APTES/NHS film

The morphology of the modified electrode was characterized by SEM analysis. It is clear from Fig. 1A that cubic structured gold nanoparticles were formed via the chemical reduction method. Fig. 1B represents the image of the GCE/AuNC/APTES modified electrode, from which energy-dispersive X-ray spectroscopy (EDX) (Fig. 1C) and elemental mapping (Fig. 1D) of Au were measured. Fig. 1E shows the ATR-FTIR spectra of AuNC (upper line) and AuNC-APTES-NHS film (lower line). The prominent peaks for AuNC spectra at 1603 cm^{-1} suggest stretching vibrations (N–H) in gold nanoparticles reported by earlier researchers. The presence of aromatic C–H stretching on the nanoparticle surface was observed by the weak overtone band at 2041 cm^{-1}. On the other hand, in the lower line, the amide-conjugated carbonyl group and methylene scissoring vibrations were characterized by the bands at 11,89 cm^{-1} and 1276 cm^{-1}. Besides, the strong band at 1070 cm^{-1} assigned to C–N stretching vibrations of aliphatic amines.

3.2. Electrochemical characterization of the modified biosensor

Cyclic voltammetry was performed in 0.1 molL^{-1} KCl including 5.0 × 10^{-3} molL^{-1} $[Fe(CN)_6]^{3-/4-}$ to modify the GC electrode surface at each modification step (Fig. 2A). The oxidation peak current of the GCE/AuNC electrode (Fig. 2Aii) was significantly increased compared to the bare GC electrode (Fig. 2Ai). The deposition of AuNC was played an electron transfer enhancer on the GCE surface. The self-redox peak was increased distinctly after added APTES (Fig. 2Aiii) and NHS (Fig. 2Aiv) crosslinker with the GCE/AuNC platform. The conducting polymer

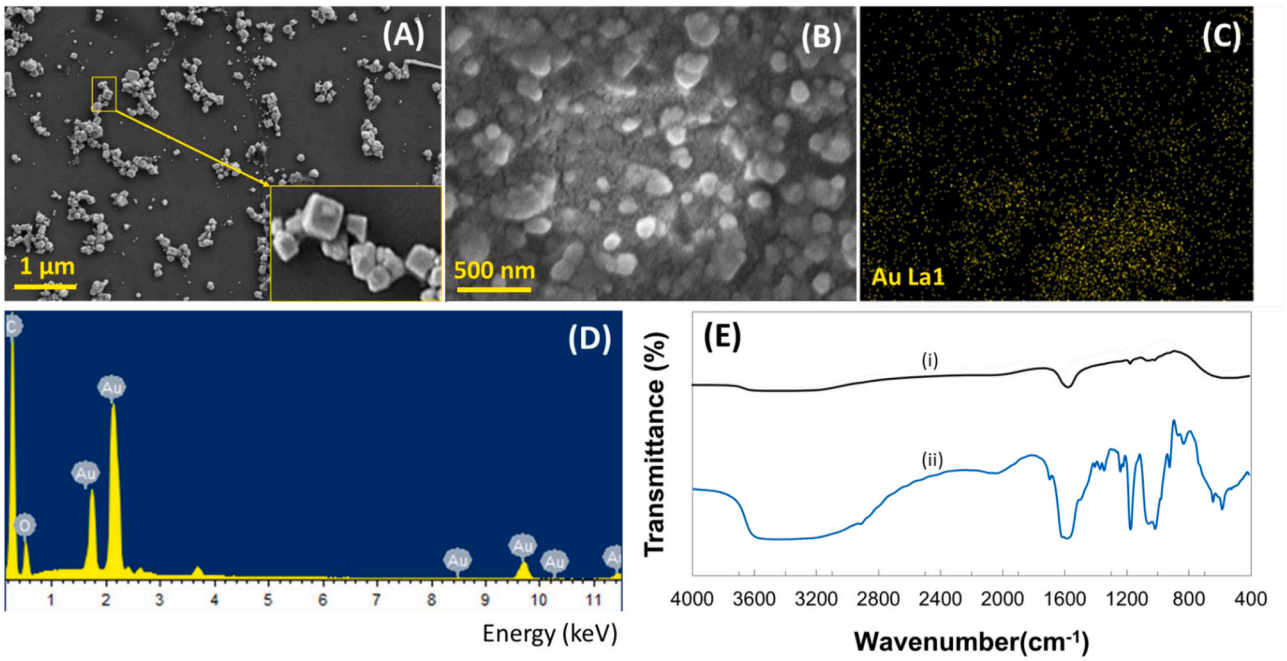

Fig. 1. SEM images of (A) as-synthesized AuNC, and (B) GCE/AuNC-APTES modified electrode. (C) The EDX spectrum of the GCE/AuNC-APTES film and (D) corresponding element mapping shows the distribution of Au nanoparticles. (E) ATR-FTIR spectrum of (i) AuNC and (ii) AuNC-APTES-NHS film.

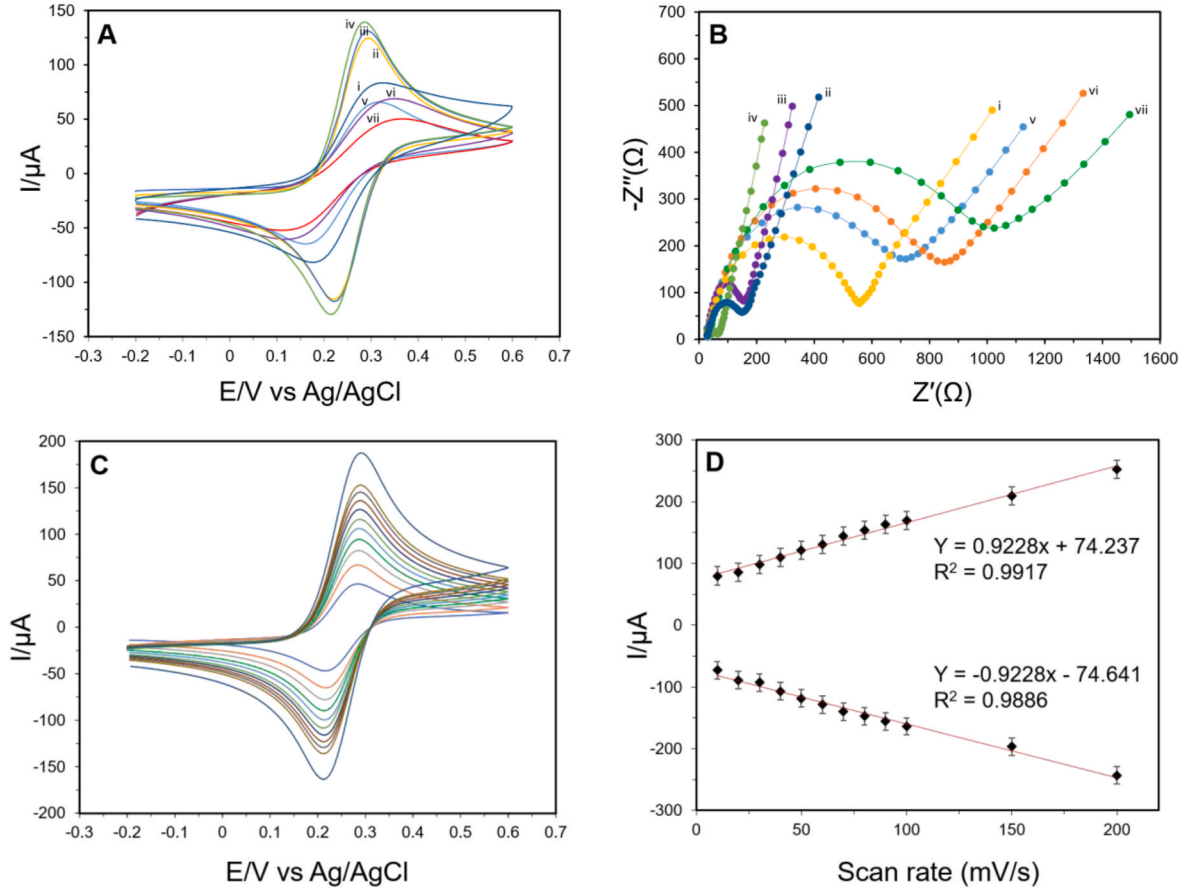

Fig. 2. Cyclic voltammograms (A) and Nyquist plot of EIS (B) of the different electrodes measured in 0.1 molL^{-1} KCl including 5.0 × 10^{-3} molL^{-1} $[Fe(CN)_6]^{3-/4-}$: (i) bare GCE, (ii) GCE/AuNC, (iii) GCE/AuNC/APTES, (iv) GCE/AuNC/APTES/NHS, (v) GCE/AuNC/APTES/NHS/CP, (vi) GCE/AuNC/APTES/NHS/CP/LT and (vii) GCE/AuNC/APTES/NHS/CP/LT/RP. (C) CV response obtained for GCE/AuNC/APTES sensor at different scan rates (from inner to outer): 10, 20, 30, 40, 50, 60, 70, 80, 90, 100, 150 and 200 mV/s in 0.1 molL^{-1} KCl including 5.0 × 10^{-3} molL^{-1} $[Fe(CN)_6]^{3-/4-}$ and (D) the corresponding calibration plots between different scan rates versus anodic and cathodic peak current.

APTES covalently attached rapidly with the AuNC and effectively enhanced the electron transfer efficiency. After immobilization of capture probe ssDNA, the oxidation peak current was decreased notably (Fig. 2Av). The loading of the non-conductive capture probe blocks the electron transfer path (Cai et al., 2021; Huang et al., 2015). The same decline trend was observed after hybridization with VCvrra linear target (Fig. 2Avi) and the reporter probe DNA (Fig. 2Avii) with the capture probe due to the formation of negatively charged double-stranded DNA and generation of repulsive within the redox probes (Chen et al., 2019; Peng et al., 2012).

The electrochemical effectiveness of AuNC/APTES to fabricate the *V. cholerae* pathogen detection was determined by EIS response (Fig. 2B). The Nyquist plot of bare GCE (Fig. 2Bi) is comparatively much bigger than that of the GCE/AuNC electrode (Fig. 2Bii), indicating an electroactive layer is formed on the GCE electrode after loading AuNC. The EIS semicircles of both APTES (Fig. 2Biii) and NHS (Fig. 2Biv) were found relatively smaller than the GCE/AuNC electrode, which confirms the positive influence of electrochemical charge transfer phenomena and reduced the charge transfer resistance (R_{ct}) value. After immobilization of the capture probe (Fig. 2Bv), the Nyquist circle was massively bigger than the GCE/AuNC/APTES/NHS electrode, which means that the loading of the non-conductive ssDNA probe increased the R_{ct} value. After deposition of a more non-conductive linear target (Fig. 2Bvi) and the reporter probe (Fig. 2Bvii) increased the charge transfer resistance (R_{ct}).

The effect of scan rate on the current response of the GCE/AuNC/APTES was confirmed by a series of CVs analysis of the redox probe (5×10^{-3} molL^{-1} $[Fe(CN)_6]^{3-/4-}$ containing 0.1 molL^{-1} KCl) at different scan rate of 10, 20, 30, 40, 50, 60, 70, 80, 90, 100, 150, 200 mV/s in the potential range of −0.2 V–0.6 V which is shown in Fig. 2C. Fig. 2D depicts a linear relationship between the scan rate and oxidation, and reduction peak current suggests adsorption controlled on the surface of the modified electrode.

3.3. Optimization condition for detection of VC

Optimization of different parameters for electrochemical measurements was essential for achieving the better performance of biosensors. For this purpose, the pH and crosslinking period of NHS was optimized via DPV measurement of 1×10^{-8} molL^{-1} and 1×10^{-6} molL^{-1} LT at the presence of 5×10^{-3} molL^{-1} AQMS.

The effect of pH on LT hybridization and electrochemical response of VC in 5×10^{-3} molL^{-1} AQMS containing 0.01 molL^{-1} PBS was recorded and shown in Fig. 3A. The result of this analysis showed the hybridization of LT was dependent on the pH of the solution. Hybridization of LT became poor at acidic conditions due to protonation of phosphate backbone and compressive stress of LT (Ulianas et al., 2014; Zhang et al., 2012). Moreover, the current responses of LT were decreased with increasing pH at basic conditions suggesting the breakage of hydrogen bond nucleotide base pairs at higher pH due to the addition of NaOH for

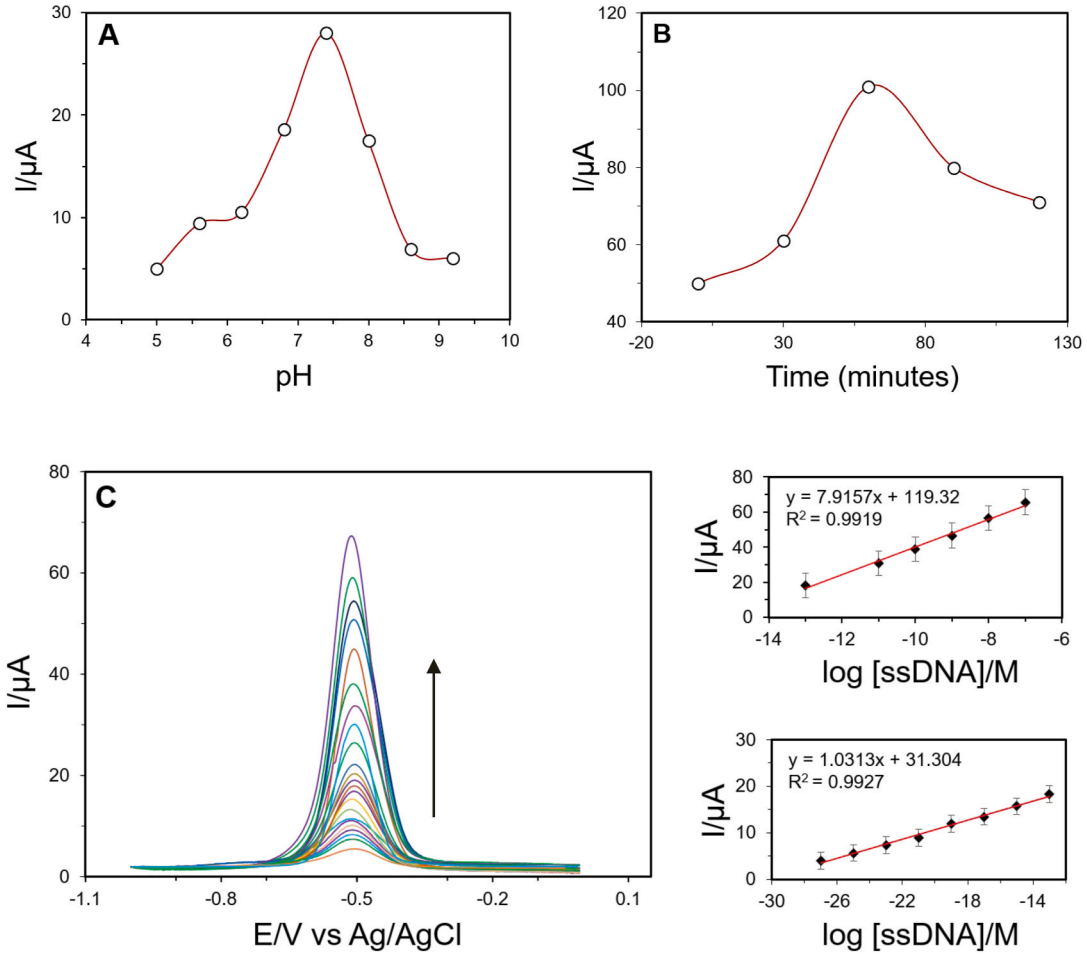

Fig. 3. The effect of pH (A) on LT hybridization and sensing response performed with 10^{-8} molL^{-1} ssDNA, the effect of NHS crosslinking periods (B) on the DNA biosensor response performed with 1×10^{-6} molL^{-1} ssDNA **(C)** DPV response curve of GCE/AuNC/APTES/NHS/CP after hybridization with 1×10^{-27} to 1×10^{-7} molL^{-1} linear target ssDNA in 0.01 molL^{-1} phosphate buffer containing 1×10^{-3} molL^{-1} AQMS at a scan rate of 100 mV/s. The condition of DPV measurements was initial potential −1 V, end potential 0 V, pulse width 50 ms, modulation 50 mV, and pulse period 0.1 s. The right-side inset graph shows the corresponding calibration curves of peak currents vs logarithm of linear target ssDNA concentrations.

pH adjustment (Rahman et al., 2017). The highest peak response was found at pH 7.4, which means a favorable condition for hybridization creates this pH.

The optimization of the crosslinking period of NHS was carried by using DPV of GCE/AuNC/APTES/NHS/CP (Fig. 3B). The Figure revealed that the DPV responses were gradually enhanced with increasing the crosslinking periods, and the highest current response was found at 1 h.

3.4. Analytical performance of modified electrode

The electrochemical activity of the AuNC/APTES modified GCE electrode was analyzed at multiple concentrations of *V. cholerae* complementary sequences using the DPV methods of AQMS oxidation response (Fig. 3C). The increasing oxidation currents of DPV signals between before- and after-hybridization were considered as the measurement signal. The calibration curves confirmed that the oxidation current of DPV exhibits two linear segments with the logarithm of the concentration of *V. cholerae* target sequence within 1×10^{-7} molL^{-1} to 1×10^{-13} molL^{-1} ($R^2 = 0.9919$) and 1×10^{-13} molL^{-1} to 1×10^{-27} molL^{-1} ($R^2 = 0.9927$). The detection limit (S/N = 3) was determined to be 7.41×10^{-30} molL^{-1} (determined from the equation of 3 b/m, b is the standard deviation of the DPV response of 5×10^{-3} molL^{-1} AQMS solution and m is the slope of the calibration curve). The sensitivity of the proposed sensor was determined 0.62 μA/nmolL^{-1}/cm^{-2} estimated from the slope of linearity data, which much lower than previously reported literature (Low et al., 2017; Patel et al., 2012; Solanki et al., 2011). The broad linear response range of *V. cholerae* biosensors can be characterized to the AuNC/APTES nanocrystalline nanocomposite particles as carrier matrices for the maximum number of probe DNA immobilization on the GCE surface. The amino group-rich layer on the AuNC/APTES nanocomposite surface is an effectively suitable binding surface for the amine-modified DNA capture probes resulted in naturally occurring covalent bond formation between the constituents. The construction of a nano-platform of AuNC with APTES resulted in a synergistic effect that enhanced the analytical performance of the DNA hybridization response, which significantly increased the sensitivity of the proposed *V. cholerae* biosensor. The wide linear response range and LOD value of the proposed biosensor confirm the effectiveness in the application field (Low et al., 2017; Patel et al., 2012; Rahman et al., 2017; Solanki et al., 2011) (Table 1).

3.5. Specificity and longtime stability of the biosensor

The specificity of the biosensor was evaluated by comparing the relative DPV response of one base mismatch, two base mismatch, NCLT, and LT shown in Fig. 4A. As can be seen in Fig. 4A, the current response of 1×10^{-7} molL^{-1} of one base mismatch, two base mismatch and NCLT are 36.63%, 20.7%, and 7.92% of the same concentration LT under the same optimized condition.

Furthermore, the stability of the proposed biosensor was investigated under the optimized conditions of DPV and was recorded for LT (1×10^{-7} molL^{-1}) in 0.01 molL^{-1} PBS presence of 5×10^{-3}molL^{-1} AQMS at a scan rate of 0.1 V^{-1}. The DPV response of GCE/AuNC/APTES/NHS/CP (Fig. 4B) was examined via LT hybridization over 30 days and checked every 7 days while being stored in a refrigerator at 4 °C. After 21 days of storage, no significant deviation (less than 3%) in peak current was found, and 24.68% deviation was calculated after one month of storage revealed the stability of the biosensor.

3.6. Reusability and reproducibility of the DNA biosensor

A three steps method was followed to confirm the reusability of the proposed biosensor. First of all, the LT of 1×10^{-7} molL^{-1} was immobilized on the surface of GCE/AuNC/APTES/NHS/CP and DPV measurement was carried similar way as discussed earlier. Secondly, immersed the LT immobilized electrode in 0.1 molL^{-1} NaOH for 5min to remove bound LT. At last, the electrode was dipped into the exact solution of LT and DPV measurement was investigated to determine the deviation of current response (if any). After four consecutive reusability studies, a smaller deviation in DPV response was found, but the deviation has become larger after 5 to 6 times reuse suggesting the covalent bond between NHS and CP may be detached during NaOH treatment (Ulianas et al., 2014) which represented in Fig. 4C. To investigate the reproducibility, sequential DPV of AQMS in the presence of 1×10^{-6} molL^{-1} target ssDNA was performed using a similarly modified electrode. It was observed that less than 1% deviation of current response of samples reveals the biosensor had an excellent reproducibility.

3.7. Analytical ability of the proposed biosensor for detection of *V. cholerae* in real sample

The analytical performance of the biosensor was also evaluated by detecting *V. cholerae* DNA with the presence of *Salmonella enterica* serovar Typhimurium (*S. typhimurium*). DPV of different concentrations of *V. cholerae* DNA were recorded for this experiment and shown in Fig. 4D. The biosensor was responsive over a *V. cholerae* concentration range of 1×10^8 CFU/ml to 1 CFU/ml and linear over the range of 1×10^8 CFU/ml to 10 CFU/ml with a regression value of 0.9861 and the lowest detectable limit of 1 CFU/ml. So, the biosensor was applicable in the detection and quantification of *V. cholerae* in mixed cultures.

To access the specificity of the biosensor in the real sample, DPV of 5 ng/μl DNA of various stains (cultured *S. typhimurium, Enterobacter acrogens*), two *V. cholerae strains*, two closely relative species (*Vibrio* spp. other than *V. cholerae*) were carried out, which is presented in Table 2. The DPV response of two *V. cholerae* was highest than others. The current response of *E. acrogens* and *S. typhimurium* were similar to the background, which revealed those two pathogens were not detected by the proposed sensor. But the current response of those relative vibrios was 11.86 and 20.83% which depicted those vibrios were detected at their higher concentration. Thus an electrochemical response less than 18.27 ± 0.25 μA can be further resolved and interpreted as non-cholerae vibrios if the response is sustained even with pure culture.

Table 1
Performance comparisons of various electrochemical DNA biosensor reported in literature for detection of *V. cholerae*.

Immobilization matrix	Analyte	Dynamic concentration range	LOD	Detection Method	Reference
ZrO_2/ITO	Complementary and genomic DNA	10^{-10} to 10^{-17} (molL^{-1})	10^{-17} (molL^{-1})	Electrochemical	Solanki et al. (2011)
Au electrode	Genomic DNA	500 to 100 ng/μl	100 ng/μl	Electrochemical	Patel et al. (2012)
Carbon electrode	Non-protein coding small RNA	–	6×10^{-17} (molL^{-1})	Electrochemical	Vijian et al. (2016)
PSA/AuNP/SPE	Complementary DNA	10^{-8} to 10^{-17} (molL^{-1})	10^{-21} (molL^{-1})	Electrochemical	Rahman et al. (2017)
Latex-AuNP/α- FTIC/SPE	Genomic DNA	–	0.5 ng/ml	Electrochemical	Low et al. (2017)
NHS/APTES/AuNC/GCE	Complementary ssDNA	10^{-8} to 10^{-14} and 10^{-14} to 10^{-27} (molL^{-1})	7.41×10^{-30} (molL^{-1})	Electrochemical	This work

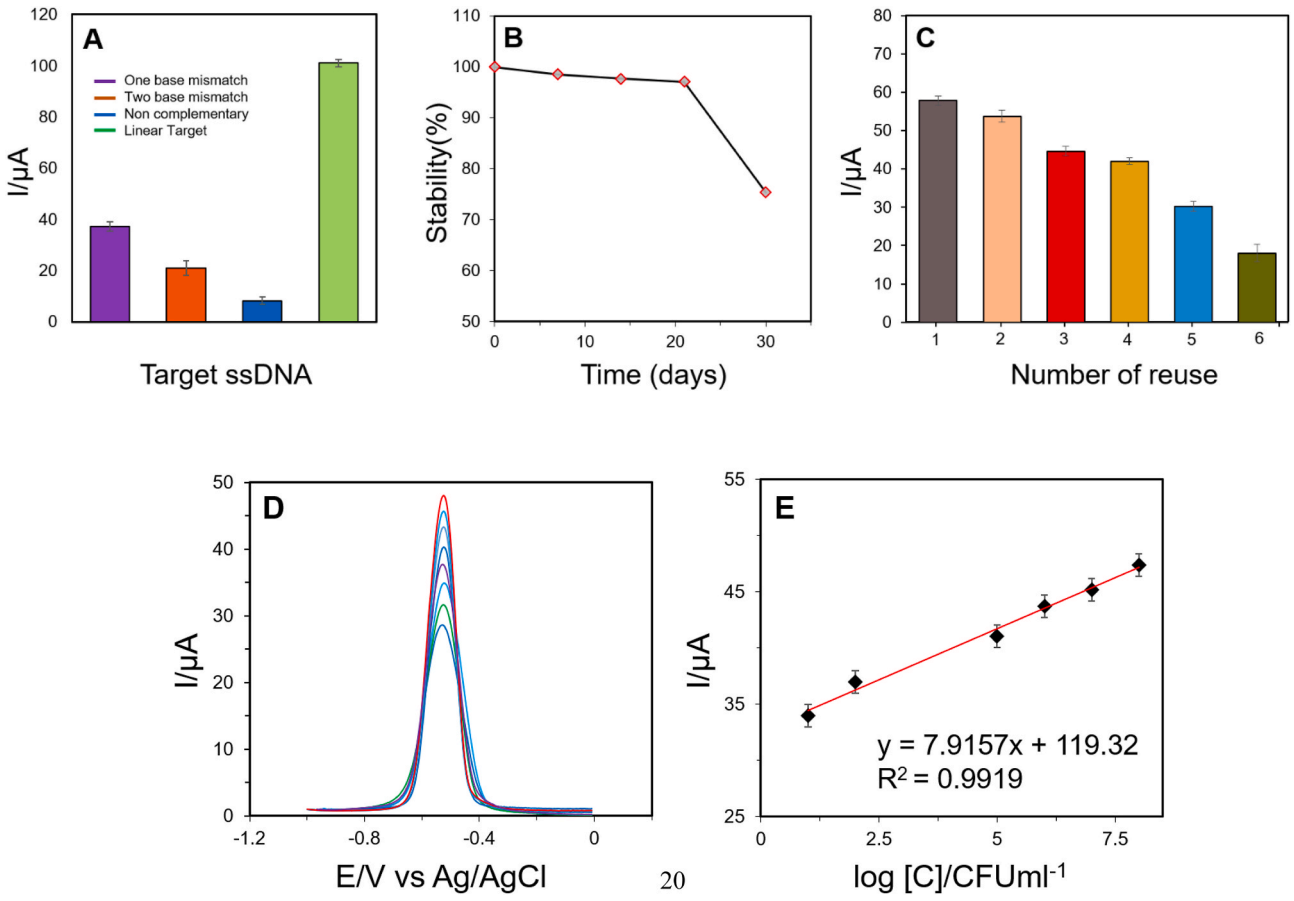

Fig. 4. (A) Current response of different target ssDNA, (B) Stability profile of GCE/AuNC/APTES/NHS/CP towards storage periods, and (C) Reusability analysis of the DNA biosensor using 0.1 molL^{-1} NaOH. All experiments were performed with 5 × 10^{-3} molL^{-1} AQMS in 0.01 molL^{-1} PBS. Electrochemical response to different concentration of *V. cholerae* in real samples (D) DPV for 5 × 10^{-3}molL^{-1} AQMS and (E) calibration plot of DPV response.

Table 2
Selectivity of DNA biosensor towards detection of *V. cholerae* in real sample.

Name of pathogens	Concentration of DNA (ng/μl)	Current response of pathogens (μA) (average ± SD)	Current response of control (μA) (average ± SD)	Percentage current response (%)	*t*-test	Remark
S. typhimurium	5.00	4.31 ± 0.42	3.87 ± 0.34	4.91	0.0001	×
V. cholerae	5.00	87.70 ± 2.62	3.87 ± 0.34	100.00	0.0251	✓
V. cholerae	5.00	87.13 ± 0.87	3.87 ± 0.34	99.35	0.0038	✓
V. spp. (other than *V. cholerae*)	5.00	18.27 ± 0.25	3.87 ± 0.34	20.83	0.0002	✓
V. mimicus	5.00	10.40 ± 1.18	3.87 ± 0.34	11.86	0.0002	✓
E. acrogenes	5.00	3.65 ± 0.36	3.87 ± 0.34	4.17	0.0001	×

√-DPV peak current is significantly higher than the control's response. × – DPV peak current is significantly lower than the control's response at 95% confidence level and 4 degrees of freedom.

3.8. Application of the biosensor for industrial purpose

V. cholerae usually transmitted in humans through food and water. Being a salt-tolerant and indigenous species in the marine environment, the bacterium can easily access the human via water (Mookerjee et al., 2015) and kinds of seafood. In poultry industries, marine dry fish is used as cheap protein sources in the feed formulation and hence to be considered the source of *V. cholerae* in poultry meats and meat products. We thought inexpensive and prompt monitoring of *V. cholerae* in the poultry industry and considered the poultry feces (litter) as a sample. Our method has successfully recovered and detected the target ssDNA fragments from spiked litter samples. The percentage of the recovery that was exhibited by the biosensor was 96.42–99.11% (shown in Table 3), which means the impurities in feces did not influence the electrochemical responses of the DNA biosensor.

Table 3
Recovery test of spiked *V. cholerae* DNA in poultry feces by using proposed DNA biosensor.

Added concentration (ng/ml)	Peak current (μA) (average ± SD)	Found concentration (ng/ml) (average ± SD)	RSD	Recoveries (%)
5.000	88.433 ± 0.759	4.821 ± 0.019	0.858	96.42
0.500	62.9 ± 0.510	0.496 ± 0.004	0.811	99.11

4. Conclusion

In summary, a DNA biosensor has been developed for efficient and sensitive detection of the most devastating *V. cholerae* epidemic bacterial pathogen. The proposed modified GCE- DNA carrier matrix sensor displayed excellent performance with high sensitivity toward *V. cholerae* detection with a LOD value of 7.41×10^{-30} molL^{-1}. This high sensitivity is an essential requirement for early clinical diagnosis of pandemic disease caused by pathogenic *V. cholerae* bacteria. The biosensor shows high selectivity in the presence of mixed bacterial samples at its lowest measurable concentration limit. Successful recovery values obtained after spiking of *V. cholerae* in poultry feces indicate the designed biosensor can be an effective tool for real-time monitoring of infections in poultry industry. In future, this finding could provide an efficient amplification approach for detecting other pathogenic bacteria as well and would be of great value for future applications in public and environmental safety. We believe this work will open a new window of opportunities for the potential application in the point-of-care diagnosis of *V. cholerae* infection in cholera epidemic countries. This unique system is expected to contribute to the development of user-friendly and portable biosensor by miniaturizing the electrochemical detection device in near future.

Author contributions

M.Z.H. Khan planned the work and designed the experiment. M. R. Ali, M. S. Bacchu and M. A. A. Shetu carried out experimental work. S. Akter supervised microbiology part of this experiment. M. N. Hasan, F. T. Chowdhury synthesized nano materials. M. M. Rahman and M. S. Ahommed performed calculated data and have written some part of the manuscript.

Declaration of competing interest

The authors declare that they have no known competing interests or personal relationships that could have appeared to influence the work reported in this paper.

Acknowledgment

The work has been done with the financial support from the Ministry of Information and Communication Technology, Government of Bangladesh (Innovation Fund).

Appendix A. Supplementary data

Supplementary data to this article can be found online at https://doi.org/10.1016/j.bios.2021.113338.

References

Alam, M., Hasan, N.A., Sultana, M., Nair, G.B., Sadique, A., Faruque, A.S.G., Endtz, H.P., Sack, R.B., Huq, A., Colwell, R.R., Izumiya, H., Morita, M., Watanabe, H., Cravioto, A., 2010. J. Clin. Microbiol. 48, 3918–3922.
Ali, M., Nelson, A.R., Lopez, A.L., Sack, D.A., 2015. PLoS Neglected Trop. Dis. 9.
Andrews, J.R., Basu, S., 2011. Lancet 377, 1248–1255.
Aulet, O., Silva, C., Fraga, S.G., Pichel, M., Cangemi, R., Gaudioso, C., Porcel, N., Jure, M. A., De Castillo, M.C., Binsztein, N., 2007. Rev. Soc. Bras. Med. Trop. 40, 385–390.
Baron, S., Chevalier, S., Lesne, J., 2007. J. Health Popul. Nutr. 25, 312–318.
Cai, R., Zhang, Z., Chen, H., Tian, Y., Zhou, N., 2021. Sensor. Actuator. B Chem. 326, 128842.
Carter, R.M., Mekalanos, J.J., Jacobs, M.B., Lubrano, G.J., Guilbault, G.G., 1995. J. Immunol. Methods 187, 121–125.
Chen, D., Zhang, M., Ma, M., Hai, H., Li, J., Shan, Y., 2019. Anal. Chim. Acta 1078, 24–31.
Chowdhury, G., Joshi, S., Bhattacharya, S., Sekar, U., Birajdar, B., Bhattacharyya, A., Shinoda, S., Ramamurthy, T., 2016. Front. Microbiol. 7, 144.
Cooper, K.L.F., Luey, C.K.Y., Bird, M., Terajima, J., Nair, G.B., Kam, K.M., Arakawa, E., Safa, A., Cheung, D.T., Law, C.P., Watanabe, H., Kubota, K., Swaminathan, B., Ribot, E.M., 2006. Foodb. Pathog. Dis. 3, 51–58.
Faruque, S.M., Albert, M.J., Mekalanos, J.J., 1998. Microbiol. Mol. Biol. Rev. 62, 1301–1314.
Goel, A.K., Ponmariappan, S., Kamboj, D.V., Singh, L., 2007. Folia Microbiol. (Praha) 52, 81–85.
Hall-Stoodley, L., Costerton, J.W., Stoodley, P., 2004. Nat. Rev. Microbiol. 2, 95–108.
Harris, J.B., LaRocque, R.C., Qadri, F., Ryan, E.T., Calderwood, S.B., 2012. Cholera. In: The Lancet. Elsevier B.V., pp. 2466–2476
Huang, H., Bai, W., Dong, C., Guo, R., Liu, Z., 2015. Biosens. Bioelectron. 68, 442–446.
Huq, A., Haley, B.J., Taviani, E., Chen, A., Hasan, N.A., Colwell, R.R., 2012. Curr. Protoc. Microbiol. 26, 6A.5.1–6A.5.51.
Khan, M.Z.H., Ahommed, M.S., Daizy, M., 2020. RSC Adv. 10, 36147–36154.
Khan, M.Z.H., Liu, Xiaoqiang, Zhu, J., Ma, F., Hu, W., Liu, Xiuhua, 2018. Biosens. Bioelectron. 108, 76–81.
Kumar, N., Hu, Y., Singh, S., Mizaikoff, B., 2018. Analyst 143, 359–373.
Kurinomaru, T., Kojima, N., Kurita, R., 2019. Curr. Protoc. Nucleic Acid Chem. 77.
Li, J., Wang, H., Zhao, Y., Cheng, L., He, N., Lu, Z., 2001. Sensors 1, 53–59.
Liew, P.S., Lertanantawong, B., Lee, S.Y., Manickam, R., Lee, Y.H., Surareungchai, W., 2015. Talanta 139, 167–173.
Liu, Y., Gong, Z., Morin, N., Pui, O., Cheung, M., Zhang, H., Li, X.F., 2006. Anal. Chim. Acta 578, 75–81.
Low, K.F., Zain, Z.M., Yean, C.Y., 2017. Biosens. Bioelectron. 87, 256–263.
Mookerjee, S., Batabyal, P., Sarkar, M.H., Palit, A., 2015. PloS One 10, e0137338.
Okada, K., Chantaroj, S., Taniguchi, T., Suzuki, Y., Roobthaisong, A., Puiprom, O., Honda, T., Sawanpanyalert, P., 2010. Diagn. Microbiol. Infect. Dis. 66, 135–139.
Patel, M.K., Solanki, P.R., Khandelwal, S., Agrawal, V. V., Ansari, S.G., Malhotra, B.D., 2012. Institute of Physics Publishing, p. 012009.
Patel, M.K., Solanki, P.R., Kumar, A., Khare, S., Gupta, S., Malhotra, B.D., 2010. Biosens. Bioelectron. 25, 2586–2591.
Peng, H., Pan, B., Wu, M., Liu, Y., Zhang, D., Xing, B., 2012. J. Hazard Mater. 233–234, 89–96.
Rahman, M., Heng, L.Y., Futra, D., Ling, T.L., 2017. Nanoscale Res. Lett. 12, 474.
Ramamurthy, T., Bhattacharya, S.K., Uesaka, Y., Horigome, K., Paul, M., Sen, D., Pal, S. C., Takeda, T., Takeda, Y., Nair, G.B., 1992. J. Clin. Microbiol. 30, 1783–1786.
Rashid, J.I.A., Yusof, N.A., 2017. Sens. Bio-Sensing Res. 16, 19–31.
Ringe, E., McMahon, J.M., Sohn, K., Cobley, C., Xia, Y., Huang, J., Schatz, G.C., Marks, L. D., Van Duyne, R.P., 2010. J. Phys. Chem. C 114, 12511–12516.
Ross, A.G.P., Crowe, S.M., Tyndall, M.W., Petersen, E., 2015. Int. J. Infect. Dis. 38, 89–94.
Shin, O.S., Tam, V.C., Suzuki, M., Ritchie, J.M., Bronson, R.T., Waldor, M.K., Mekalanos, J.J., 2011. MBio 2.
Solanki, P.R., Patel, M.K., Kaushik, A., Pandey, M.K., Kotnala, R.K., Malhotra, B.D., 2011. Electroanalysis 23, 2699–2708.
Tarr, C.L., Patel, J.S., Puhr, N.D., Sowers, E.G., Bopp, C.A., Strockbine, N.A., 2007. J. Clin. Microbiol. 45, 134–140.
Teschler, J.K., Zamorano-Sánchez, D., Utada, A.S., Warner, C.J.A., Wong, G.C.L., Linington, R.G., Yildiz, F.H., 2015. Nat. Rev. Microbiol. 13, 255–268.
Ulianas, A., Heng, L.Y., Ahmad, M., Lau, H.Y., Ishak, Z., Ling, T.L., 2014. Sensor. Actuator. B Chem. 190, 694–701.
Vijian, D., Chinni, S.V., Yin, L.S., Lertanantawong, B., Surareungchai, W., 2016. Biosen. Bioelectron. 77, 805–811.
Weil, A.A., Khan, A.I., Chowdhury, F., LaRocque, R.C., Faruque, A.S.G., Ryan, E.T., Calderwood, S.B., Qadri, F., Harris, J.B., 2009. Clin. Infect. Dis. 49, 1473–1479.
Xu, S., Zhang, Y., Dong, K., Wen, J., Zheng, C., Zhao, S., 2017. Int. J. Electrochem. Sci. 12, 3443–3458.
Yamazaki, W., Seto, K., Taguchi, M., Ishibashi, M., Inoue, K., 2008. BMC Microbiol. 8, 94.
Yu, C.Y., Ang, G.Y., Chua, A.L., Tan, E.H., Lee, S.Y., Falero-Diaz, G., Otero, O., Rodríguez, I., Reyes, F., Acosta, A., Sarmiento, M.E., Ghosh, S., Ramamurthy, T., Yean Yean, C., Lalitha, P., Ravichandran, M., 2011. J. Microbiol. Methods 86, 277–282.
Yu, C.Y., Ang, G.Y., Chan, K.G., Banga Singh, K.K., Chan, Y.Y., 2015. Biosens. Bioelectron. 70, 282–288.
Zhang, J., Lang, H.P., Yoshikawa, G., Gerber, C., 2012. Langmuir 28, 6494–6501.
Zheng, F., Wang, P., Du, Q., Chen, Y., Liu, N., 2019. Front. Chem. 7, 232.